Analyst

PAPER

View Article Online
View Journal

Cite this: DOI: 10.1039/c6an00264a

Investigation of an SPR biosensor for determining the influence of connexin 43 expression on the cytotoxicity of cisplatin†

Yijia Wang,[a] Shiwu Zhang,[a] Chunze Zhang,[a] Zhenying Zhao,[a] Xiaoli Zheng,[a] Lihua Xue,[a] Jun Liu*[a] and X.-C. Yuan*[b]

Received 2nd February 2016,
Accepted 20th April 2016

DOI: 10.1039/c6an00264a

www.rsc.org/analyst

The real-time and label free detection abilities of surface plasmon resonance (SPR) biosensors provide a way of evaluating the influence of some genes' expression on anti-tumor drug cytotoxicity. However, studies in this field are lacking. Connexin 43 is a tumor suppressor gene and the mechanism of its effect in cisplatin cytotoxicity is still unclear. A phase SPR biosensor was used to determine the influence of connexin 43 expression on cisplatin cytotoxicity in three cancer cell lines. The results showed that the SPR signal curves have two stages. In the first hour, the SPR signal shows dramatic changes which are related to connexin 43 expression. In the subsequent stage, the SPR signal slowly declines and is related to apoptosis. Comparison of SPR measurements from several conventional biological assays showed that connexin 43 expression can affect cellular response to cisplatin in the period of oxidative stress, and results in the cells being more sensitive to cisplatin. The conclusion is further confirmed by long-term SPR measurement results and cellular morphological changes.

1 Introduction

The surface plasmon resonance (SPR) biosensor is a valuable tool for monitoring biological reactions because of the advantages of its real-time and label free detection. The SPR biosensor has been successfully used in cytobiology for several years.[1] In a previous study, an SPR biosensor was used to measure the cellular response to the cytotoxicity of cetuximab, an anti-tumor drug.[2] However, this study only provided the initial methodology and did not include detailed analysis. Previous studies have shown that expression of some tumor suppressor genes can affect the cytotoxicity of anti-tumor drugs.[3] To the best of our knowledge, studies on the mechanisms of cytotoxicity by a method with real-time detection ability are lacking. It is speculated that the mechanism of cytotoxic response can be determined in more detail using the real-time detection ability of SPR biosensors.

Connexin 43 (Cx43) is a member of the gap junction protein family of connexins[4] and is a predictive factor for chemotherapy in many tumors.[5] Cx43 is the most expressed member of the connexin family[6] and the predominant connexin isoform in many cell types.[7,8] Connexins form an intercellular channel called gap junction intercellular communication (GJIC).[9] GJIC is permeable to a variety of cytoplasmic molecules and is involved in the cytotoxicity of several drugs.[10–13] GJIC function can be enhanced or modified by several agents[14–16] and upregulated by connexin expression. Increased Cx43 expression can sensitize many tumors to chemotherapeutic agents[17] but can also cause other tumors to become drug resistant.[18] The underlying mechanisms are still unclear. For example, cisplatin is a typical chemotherapeutic drug and its cytotoxicity is related to GJIC function,[10] but the mechanism needs to be further investigated.

In the present study, the expression of Cx43, a major protein component of GJIC, in the cytotoxicity of cisplatin was examined. The cellular response to cisplatin was also monitored and analyzed using a phase SPR biosensor.

2 Materials and methods

2.1 Reagents and antibodies

All cell culture media, trypsin and antibiotics were purchased from Gibco (Grand Island, NY, USA), and fetal bovine serum (FBS) was purchased from HyClone (Logan, UT, USA). Rabbit anti-Cx43 polyclonal antibody, rabbit anti-caspase-3 polyclonal antibody, rabbit anti-β-actin polyclonal antibody, anti-rabbit

[a]Tianjin Union Medical Center, Tianjin, 300121, China. E-mail: junliu_sci@163.com
[b]Institute of Micro & Nano Optics, Key Laboratory of Optoelectronic Devices and Systems of Ministry of Education and Guangdong Province, College of Optoelectronic Engineering, Shenzhen University, Shenzhen, 518060, China.
E-mail: xcyuan@szu.edu.cn

†Electronic supplementary information (ESI) available. See DOI: 10.1039/c6an00264a

IgG-peroxidase, Hoechst 33342, poly-L-lysine, methyl thiazolyl tetrazolium (MTT), neomycin (G418), oleamide and retinoic acid were purchased from Sigma-Aldrich (St. Louis, MO, USA). Rabbit anti-ATPase β3(Na^+/K^+) polyclonal antibody was purchased from GeneTex (Irvine, CA, USA). ProteoExtract® Native Membrane Protein Extraction Kit and Immobilon membranes were purchased from Merck Millipore (Bedford, MA, USA). G418 sulfate was purchased from Calbiochem (San Diego, CA, USA). pTARGET™ Mammalian Expression Vector was purchased from Promega (Madison, WI, USA). Lipofectamin™ Reagent, CellTracker CM-Dil and Calcein-AM were purchased from Invitrogen (Carlsbad, CA, USA). ECL Plus substrate, bicinchoninic acid (BCA) reagents and RIPA lysis buffer were purchased from CWBio (Beijing, China). Cisplatin was purchased from Qilu Pharmaceutical (Jinan, China). Reactive Oxygen Species assay kit and Caspase 3 Activity assay kit were purchased from the Beyotime Institute of Biotechnology (Shanghai, China).

2.2 Cell lines

Human non-small cell lung carcinoma cell line A549, human colorectal carcinoma cell line HCT106 and human breast duct carcinoma cell line BT549 were purchased from the Shanghai Institutes for Biological Sciences, Chinese Academy of Sciences. The A549 and HCT106 cell lines were cultured in Dulbecco's Modified Eagle medium supplemented with 10% FBS, 100 U per mL penicillin and 100 μg per mL streptomycin. The BT549 cell line was cultured in RPMI 1640 medium supplemented with 10% FBS, 100 U per mL penicillin and 100 μg per mL streptomycin.

2.3 Vector construction and transfection

The complementary DNA of the human Cx43 coding region was amplified by the polymerase chain reaction using the following primers: forward 5 forward of the human Cx43 co and reverse 5 and reverse the human Cx43 polymerase chain reaction products were purified and inserted in the pTARGET™ vector. Expression vectors were transfected into cells using Lipofectamine™ Reagent. After transfection, cultures were selected with 400 μg per mL G418. Cells of subclones were diluted and seeded to obtain further clones.

2.4 Western blot analysis

Cell membrane proteins were extracted using the ProteoExtract® Native Membrane Protein Extraction Kit according to the manufacturer's instructions. Protein content was quantitated using BCA reagents. Protein samples (50 μg) were boiled in sodium dodecyl sulfate (SDS) loading buffer, separated on SDS-polyacrylamide gel electrophoresis (PAGE) gels, and transferred to Immobilon membranes by a semi-dry blotting method. The membranes were probed with anti-Cx43 (1 : 4000 dilution) and anti-ATPase β3 primary antibodies (1 : 4000 dilution) and the anti-rabbit IgG-peroxidase secondary antibody (1 : 10 000 antibody) using standard techniques. ATPase β3 was used as a loading control. The signals were visualized using electrochemical luminescence with the ECL plus and exposed film.

2.5 "Parachute" dye coupling assay

Functional GJIC was examined as described by Hong *et al.*[10] Transfected cells were grown to confluence in 6-well plates. Two fluorescent dyes, CM-Dil and Calcein-AM, were used to determine the GJIC function. CM-Dil is a membrane dye that cannot spread to coupled cells. Calcein-AM can be converted intracellularly into the GJIC permeable dye, calcein. Donor cells in one well were stained with fresh culture medium containing 10 μg per mL Calcein-AM and 5 μg per mL CM-Dil for 30 min at 37 °C. After incubation, donor cells were washed three times with culture medium to remove unincorporated dye. Donor cells were trypsinized and seeded onto a monolayer of receiver cells grown in another well. The ratio of donor to receiver cells was 1 : 150. GJICs between donor and receiver cells were allowed to form for 4 h at 37 °C. GJIC function was measured using a fluorescence microscope (Olympus CKX41). The red fluorescence of CM-Dil was used to identify donor cells and the green fluorescence of calcein-AM was used to calculate the average number of illuminant receiver cells around each donor cell. This number was considered as a degree of GJIC function. Two GJIC regulators, retinoic acid and oleamide, were also included in these assays. Retinoic acid is a GJIC potentiator and was used at a 10 μM working concentration and oleamide is a GJIC inhibitor and was used at 25 μM working concentration.

2.6 Cisplatin treatment and MTT assay

Cisplatin stock solutions were prepared fresh at 1 mg mL^{-1} in phosphate buffered saline (PBS) and added to wild type (WT) and transfected cell lines at the following working concentrations: 2 μM in BT549 cells, 5 μM in A549 cells, and 15 μM in HCT106 cells. Cisplatin treated cells were incubated in a carbon dioxide (CO_2) incubator for 24 h.

Cells were cultured in a 96-well microtiter plate under nearly 100% culture density in which GJIC formation was possible. Oleamide and retinoic acid were used to adjust the GJIC function. The MTT assay was performed as described by Kim *et al.*[19] MTT solution (20 μL of 5 mg mL^{-1}) was added to each well 24 h after cisplatin exposure, and the cells were incubated for 4 h at 37 °C. After the supernatant was removed, 100 μL of dimethylsulfoxide was added to dissolve the crystals. After 10 min of slow vibration, the absorbance was monitored at a wavelength of 490 nm. The percentage of cell survival was calculated by defining the absorption of cells not treated with cisplatin (control) as 100%. Measurements were performed in triplicate.

2.7 Apoptosis evaluation using caspase-3 detection and Hoechst 33342 staining

Cellular apoptosis was determined using caspase-3 activation[20] and Hoechst 33342 staining assays.[21] Cleavage of caspase-3 was measured using western blot analysis.[20] Cells were harvested at 0, 3, 6, 7.5, 9, or 12 h after treatment with cispla-

tin and lysed with RIPA lysis buffer. Crude cytosol fractions were separated on a 12% SDS gel (20 μg per lane) and examined using western blot analysis. Caspase-3 antibody was used at a 1 : 4000 dilution, the anti-β-actin antibody was used at a 1 : 3000 dilution and anti-rabbit IgG-peroxidase was used at a 1 : 10 000 dilution.

Caspase-3 enzyme activity was measured using the Caspase-3 Activity Assay Kit.[20] In brief, 30 μg of the cellular total protein of each sample was incubated with 10 μl of Ac-DEVD-*p*NA (2 mM) substrate in a total volume of 100 μl of assay buffer for 1.5 h at 37 °C. *p*NA was detected using a colorimetric method at 405 nm in order to calculate the caspase-3 enzyme activity.

For staining assays, living cells were directly stained with Hoechst 33342 at a working concentration of 1 μg mL^{-1} for 20 min and then examined with a fluorescence microscope. Apoptotic cells, which have shrunken nuclei with chromatin condensation, were counted to calculate the apoptosis rate.

2.8 Measurement of intracellular reactive oxygen species

The level of intracellular reactive oxygen species (ROS) was quantified using a Reactive Oxygen Species Assay Kit.[23] Dichloro-dihydro-fluorescein diacetate (DCFH-DA) has no fluorescence signal and can be oxidized by ROS in viable cells to 2′,7′-dichlorofluorescein which is highly fluorescent at 530 nm. Cells were washed three times with serum free medium. DCFH-DA, diluted to a final concentration of 10 μM with serum free medium, was added and incubated in a 37 °C incubator for 30 min. After washing three times with PBS to remove DCFH-DA which did not enter the cells, the fluorescence intensity was measured every 2 min using a microplate reader (485 nm excitation and 535 nm emission). Cisplatin with a final concentration indicated in section 2.6 was added to the medium after a negative control period of 10 min. Rosup, a positive control supported by the kit, was used with a final concentration of 0.1 mg mL^{-1} as an external oxidant molecule. Measurements were performed in triplicate.

2.9 SPR biosensor

The differential interference phase-sensitive SPR biosensor established in a previous study[2] was used to measure the cells. Briefly, the response unit (RU) of the system, which is the phase shift caused by the SPR phenomenon, can be obtained using a Mach–Zehnder configuration. The microfluidic system has a single channel, which was bonded on a glass slide coated with a 45 nm thick gold film to fabricate the sensor chip (Fig. S1†). Through the standard molding process,[22] negative photoresist SU-8 (MicroChem) and polydimethylsiloxane (PDMS) (Dow Corning) were used to form the microfluidic channel. The channel was about 2 cm in length, 1.8 cm in width and 150 μm in height. It has a steamlined structure to avoid the occurrence of bubbles which can affect the RU level. To realize fluid circulation, both ends of the PDMS body were perforated by two fused silica capillary tubes and connected to two polytetrafluoroethene (PTFE) microbore tubes (Cole-Parmer Instrument Company) to extend the circulation. All the junctions were sealed using electronic sealant (Dow Corning) to prevent possible leakage. To meet the needs of long-term measurements, the sensitivity and stability of the system were determined to the level of 10^{-6} refractive index units (RIU) and 7.25×10^{-6} RIU, respectively, during the 6 h measurement process (Fig. S1†).

2.10 SPR analysis of cellular response to cisplatin

The sensor chip was treated with 0.02 mg mL^{-1} poly-L-lysine overnight and washed twice with Hank's balanced salt solution (137.93 mM NaCl, 5.33 mM KCl, 4.17 mM $NaHCO_3$, 0.441 mM KH_2PO_4, 0.338 mM Na_2HPO_4, 5.56 mM D-glucose). Cells were trypsinized and seeded on the chip surface coated with poly-L-lysine. For adhesion of cells onto the chip surface, the microfluidic channel was filled with culture medium and maintained at 37 °C in a 5% CO_2 incubator for 8 h. After the cells were completely adhered to the chip surface with a strength of 100%, culture medium containing cisplatin was injected to treat the cells at 20 μL min^{-1} and SPR signals were recorded for 6 h. Air conditioning was used to maintain the temperature at 37 °C. Experiments were performed in triplicate for each cell type. Cell types for SPR analysis included A549-WT, HCT106 (HCT106-WT), and BT549 (BT549-WT) cells and cells transfected with Cx43 expression vectors (A549-Cx43, HCT106-Cx43, and BT549-Cx43). For further comparison, WT and Cx43-transfected cells were photographed every 0.5 h during the 6 h process of cisplatin treatment using fluorescence microscopy (Olympus CKX41).

3 Results

3.1 Confirmation of transfection and GJIC function

Previous studies showed that expression of the Cx43 is reduced in many cancers, such as human mammary carcinoma,[24] lung cancer,[25] and colorectal cancer.[26] Therefore, A549, HCT106, and BT549 cells were selected for analysis in this study. Membrane expression of Cx43 in WT and Cx43-transfected cells was evaluated using western blotting (Fig. 1). A549-WT cells showed a detectable level of endogenous expression of Cx43 whereas HCT106-WT and BT549-WT cells showed no endogenous Cx43 expression. All transfected cell lines showed high levels of Cx43 expression.

The "Parachute" dye-coupling assay revealed a positive correlation between GJIC function and Cx43 expression (Fig. 2). All Cx43-transfected cell lines had higher levels of GJIC function than their WT counterparts. The effects of retinoic acid and oleamide on GJIC were also tested and results confirmed that retinoic acid acts as a GJIC potentiator and oleamide as a GJIC inhibitor.

3.2 Effects of GJIC on cisplatin induced cellular apoptosis

Next the effect of GJIC function in the cytotoxicity of cisplatin was determined.

MTT assays confirmed various levels of cellular apoptosis in the three WT cell lines treated with cisplatin, and all Cx43-transfected cell lines were more sensitive to cisplatin than

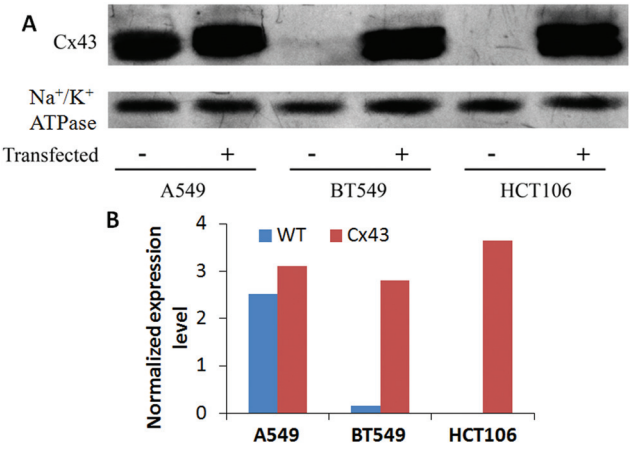

Fig. 1 Cx43 expression in the membrane of WT and Cx43-transfected cells. (A) Western blot analysis of A549, BT549, and HCT106 cell lines transfected with Cx43 expression vectors. Na^+/K^+ APTase β3 subunit served as loading control. (B) Cx43 expression level was determined using Quantity One software (Bio-Rad Laboratories) and was normalized by Na^+/K^+ ATPase expression level.

their WT counterparts (Fig. S2†). In general, retinoic acid pretreatment of Cx43-transfected cells showed higher sensitivity to cisplatin, whereas pretreatment with oleamide showed protective effects against cisplatin.

Cleaved caspase-3, caspase-3 enzymatic activity (Fig. 3 and 4) and Hoechst 33342 staining (Fig. S3†) assays showed similar results. Measurements of cleaved caspase-3 and caspase-3 enzymatic activity at various times after cisplatin treatment revealed that Cx43-transfected cell lines tended to show slightly earlier and/or increased caspase-3 activation compared with their WT counterparts. Addition of retinoic acid to Cx43-transfected cells resulted in earlier caspase-3 activation, whereas oleamide treatment resulted in delayed caspase-3 activation. Fig. S3† shows images of cells undergoing late apoptosis induced by cisplatin for 24 h as assayed by Hoechst 33342 staining. In all cisplatin treated cell types, a considerable proportion of cells displayed characteristics of apoptosis with fragmented and condensed nuclei. Furthermore, the cytotoxicity of cisplatin was associated with enhanced GJIC. Cx43-transfected cells showed higher apoptotic rates compared to WT cells, and modulation of GJIC function by retinoic acid or oleamide was also related to apoptotic rate.

3.3 GJIC enhances cisplatin induced oxidative stress

The ROS level of cells with different GJIC function were measured during cisplatin treatment. Fig. 5 shows that the ROS level was increased during the first hour of cisplatin treatment in all cells. The ROS level of the "Cx43" group was higher than that of the "WT" group in the three cell lines after cisplatin treatment. The cells of the "Cx43" group were pretreated with retinoic acid or oleamide before further analysis. Retinoic acid pretreated cells have higher ROS levels than untreated cells and oleamide pretreated cells have lower ROS levels than untreated cells.

3.4 SPR analysis of cellular response to cisplatin

Next SPR measurements of cells treated with cisplatin (Fig. 6) were performed. The RU of all cells ascended quickly in the first hour and then declined gradually over time. A peak RU value emerged at about 40 min after cisplatin treatment. Two values were determined for analyses: the RU peak value ("Max") and the difference between "Max" and RU at 6 h ("Decline"). Comparing the signal curves with previous results, the peak timing and shape of the curves showed no relation to regulator treatments, but GJIC function and regulator treatment influenced "Max" and "Decline". GJIC function contributes to cisplatin cytotoxicity based on Fig. 3–5, S2 and S3.† Comparing the signal curve results with the apoptosis assays, cells with more sensitivity to cisplatin had higher "Max" and "Decline" values, which was verified using the Student's *t* test (Fig. 6D). Next the morphologic changes of WT and Cx43-transfected cells (Fig. S4†) were examined and these findings were compared with the SPR curves. Regulators had a considerable effect on SPR signal curves in the first hour, which is during the period of oxidative stress caused by cisplatin,[27] and the morphologic changes may relate to caspase-3 activation (Fig. 7).

4 Discussion

Cx43 is an important component of GJIC and can be overexpressed in cells to upregulate GJIC.[28] Indeed, these results showed that GJIC function was upregulated in all three Cx43-transfected cell lines, even in A549 cells, which express endogenous Cx43. GJIC function of Cx43-transfected cells can be effectively adjusted by specific regulators if the regulators are added early. Thus, a system comprising cell lines was established with comparatively high or low Cx43 expression and Cx43-stimulated GJIC function that could be adjusted by regulators, allowing for further analysis and SPR measurement.

The cytotoxicity of the anti-tumor drug cisplatin can be enhanced by GJIC.[29,30] Consistent with this study, our MTT and Hoechst 33342 staining assays showed that upregulation of Cx43 expression enhanced the cytotoxicity of cisplatin. These results are similar to those obtained by Tong *et al.*[30] However, this study expanded these findings by examining the effects at later time points and in response to treatment with various regulators. The effect of Cx43 enhancement of GJIC on cisplatin cytotoxicity and the effect of GJIC regulators on cisplatin cytotoxicity were both comprehensively determined. These results can be used for comparison with the following SPR measurements.

To analyze apoptosis during the early stages, western blotting was used to detect caspase-3 cleavage in all cell types at various time points. Caspase-3 plays a direct role in apoptosis,[31] and its cleavage is widely used to indicate the stage of apoptotic progress.[32,33] Thus, cells that are more sensitive to cisplatin show earlier caspase-3 cleavage and higher cleavage

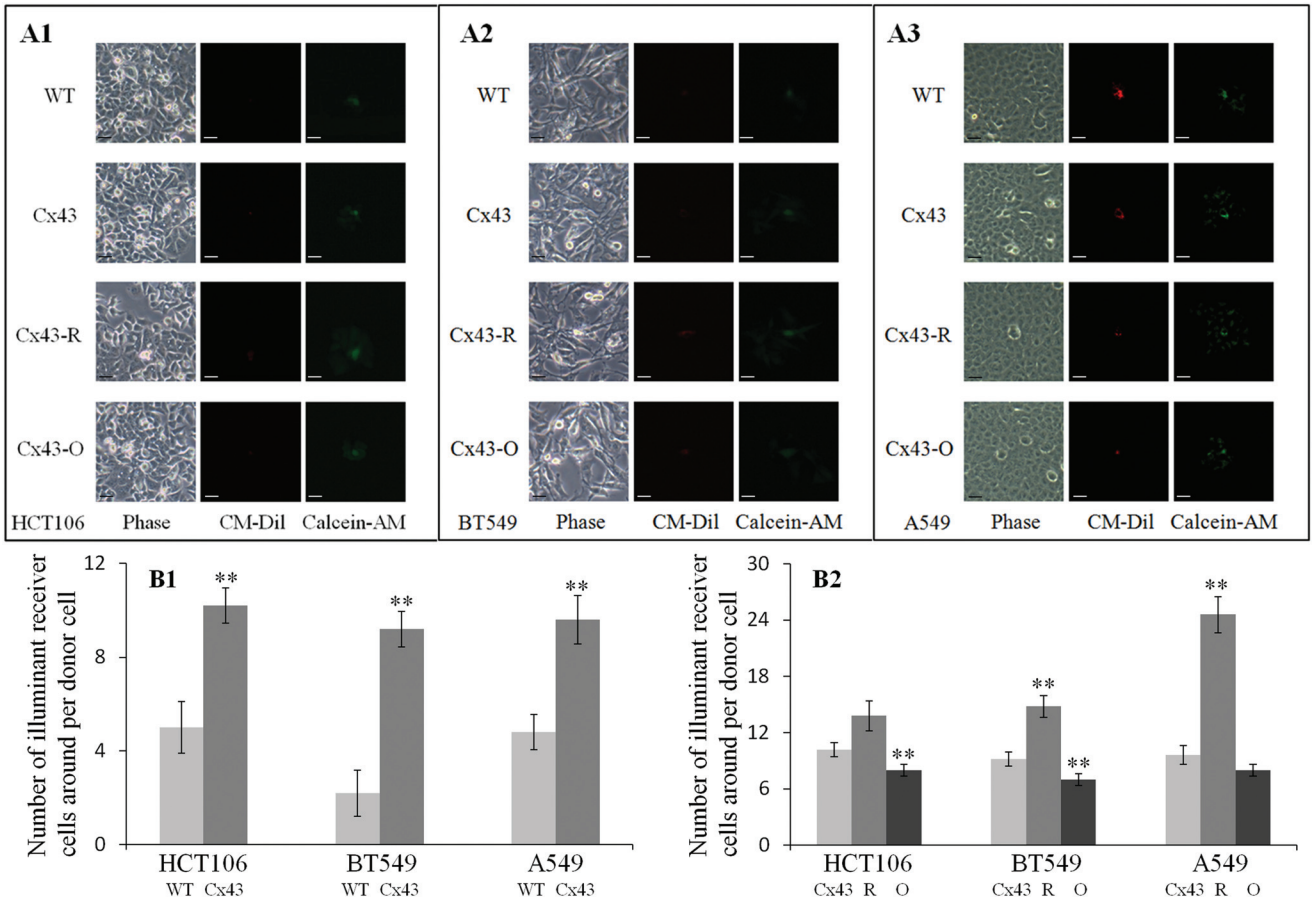

Fig. 2 "Parachute" dye-coupling assay. (A1–3) The dye transfer distances through GJIC were measured in three cell lines by "Parachute" dye coupling assays. Cells were transfected with control vectors (WT) or Cx43 expression vectors (Cx43) and treated with retinoic acid (10 μM) for 24 h or oleamide (25 μM) for 1 h before the assay. The dye transfer distance was longer in cells overexpressing Cx43 compared with WT cells. Retinoic acid treatment of Cx43-transfected cells (Cx43-R) significantly enhanced the dye coupling while oleamide treatment (Cx43-O) inhibited dye coupling. (B1–2) GJIC function in three cell lines transfected with control (WT) or Cx43 expression vectors (Cx43) or transfected with Cx43 and treated with retinoic acid (R) or oleamide (O). Columns show the mean from five independent experiments and standard deviations are shown as bars. $^{**}P < 0.05$, significantly different from the Cx43 group of the same cell line. GJIC functions of all Cx43 transfected cells were higher than WT cells. Retinoic acid and oleamide showed considerable enhancement and inhibition effects, respectively, on GJIC in Cx43-transfected cells. The scale bars represent 10 μm.

levels. The caspase-3 assays were consistent with MTT and Hoechst 33342 staining assays.

Some biological detection methods with real-time ability, such as flow cytometry or fluorescence microscopy, require radioactive labelling needed. Labelling affects the measurement results and cell viability, but the SPR biosensor is a label free method and can avoid these problems. Compared with other novel optical methods, such as optical tweezers,[34] optical stretcher[35] and deformability cytometry,[36] the SPR biosensor has better real-time ability to monitor cellular responses to drugs. The SPR biosensor can measure RIU near chip surface (about 200 nm) in real time and export data as RU, so it can be used to measure living cells. The changes of intracellular material and cellular morphology both contribute to RU variation.[1] Long stability times and high sensitivity are both needed for successful SPR applications in cytobiology, as reactions between cells and agents can require long exposure times. The SPR sensor used in this research is a phase-modulated SPR sensor based on a Mach–Zehnder configuration. Because unwanted disturbances are common to both beams of the Mach–Zehnder configuration, they can be canceled using phase subtraction.[37] The background noise can be effectively eliminated by the configuration so that the SPR sensor can discriminate samples with 10^{-6} RIU difference and has a 7.25×10^{-6} RIU stability at 6 h. These performance indices meet the requirements for cytobiology reaction measurements.

The cells for SPR measurement were cultured on a glass/gold/poly-L-lysine surface which is a widely used structure in SPR biosensors to culture cells.[1] PDMS was also a typical material used to make cell culture channels of SPR biosensors.[38] The cells without cisplatin treatment were used as control groups to exclude the effects of these artefacts on the cells. The SPR signal of the control groups decreased much slower than that of the other groups within the first 6 h during SPR measurement, so the effect of the incubation conditions can be ignored. These results showed two stages detected by

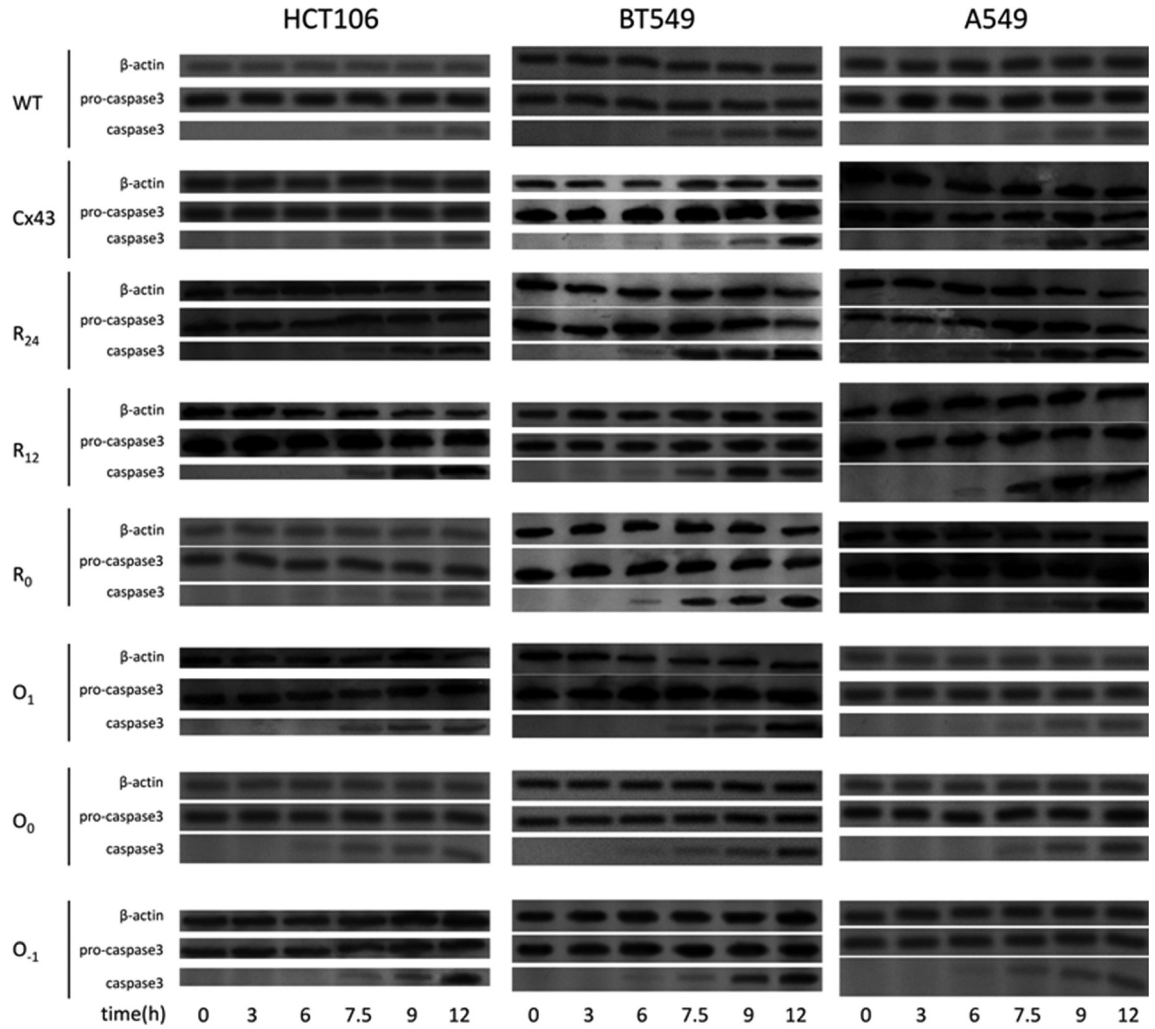

Fig. 3 Caspase-3 cleavage in response to cisplatin treatment. Western blot analysis of caspase-3 cleavage in three cell lines treated as indicated after exposure to cisplatin for the indicated times. Cells were transfected with control vector (WT) or Cx43 expression vector (Cx43). Cx43-transfected cells were treated with retinoic acid (10 μM) for 24 h before cisplatin exposure (R_{24}), 12 h before cisplatin exposure (R_{12}) or at the same time as cisplatin exposure (R_0); Cx43-transfected cells were also treated with oleamide (25 μM) 1 h before cisplatin exposure (O_1), at the same time as cisplatin exposure (O_0) or 1 h after cisplatin exposure (O_{-1}). Crude cytosol fractions (20 μg per lane) were separated on 12% SDS gels.

the SPR sensor in the cellular response to cisplatin: the initial rapid increase of RU at around 40 min, and the subsequent gradual decline of RU. Comparison of SPR measurement curves with our previous biological experiments showed that "Max" and "Decline" values are both related to GJIC function. Furthermore, cells with a higher GJIC function have higher "Max" and "Decline" values and are more sensitive to cisplatin.

The essence of real-time SPR detection curves is RIU variation of cells,[1,39] so WT and Cx43 cells were photographed using microscopy every 30 min after cisplatin treatment to compare the curves. Cells gradually shrunk and the gap between cells also gradually enlarged, suggesting that GJIC also continuously declined. However, the intercellular gap was not too wide during the time frame of the first stage to affect GJIC function, and therefore GJIC may affect cytotoxicity at the early stage of cisplatin treatment. However, decrease of RU in the second stage corresponded to these cellular morphological changes.

The large variations of RU in the first stage may be because of oxidative stress induced by cisplatin, which is one of the first responses of cells upon treatment with cisplatin.[27] GJIC is permeable to several small molecules that could be involved in cisplatin induced oxidative stress. One of these molecules is glutathione, which is a likely candidate to protect against oxidative stress[40] and has shown considerable alterations in some cancer cells in the first hour after cisplatin treatment.[41] However, GJIC can also enhance the cytotoxicity of cisplatin. For example, Ca^{2+} ions are the most probable death messengers spread through GJIC[42] and the concentration of Ca^{2+} also changes in the early stage of cisplatin treatment.[43] Thus, GJIC has two different effects on oxidative stress, and the dominant effect will determine cellular sensitivity to cisplatin. This effect is shown by the SPR measurements and is confirmed by the

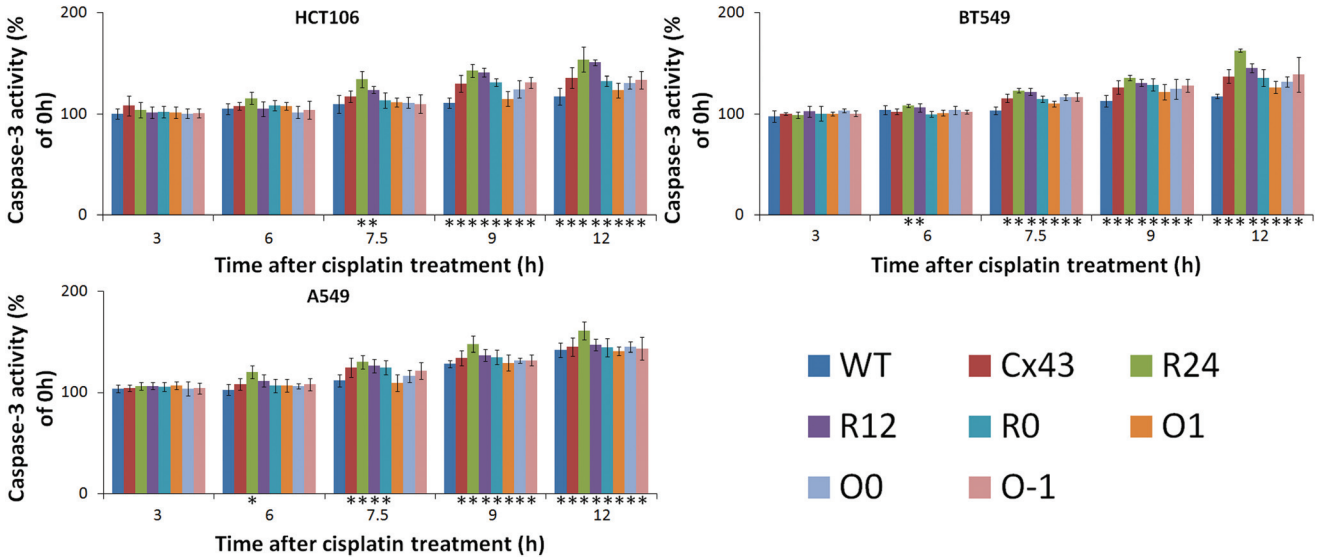

Fig. 4 Caspase-3 enzymatic activity after cisplatin treatment. After exposure to cisplatin for 0–12 h, the caspase-3 activity in the three cell lines was determined by measuring the amount of *p*-nitroaniline (*p*NA) resulting from cleavage of the conjugated substrate (Ac-DEVD-*p*NA). A standard curve and a colorimetric assay were used to determine relative protease activity of caspase-3. The activation index was determined as the ratio between the activity in treated cells and untreated cells (0 h, which is not shown in the figure). **P* < 0.05, compared with untreated cells.

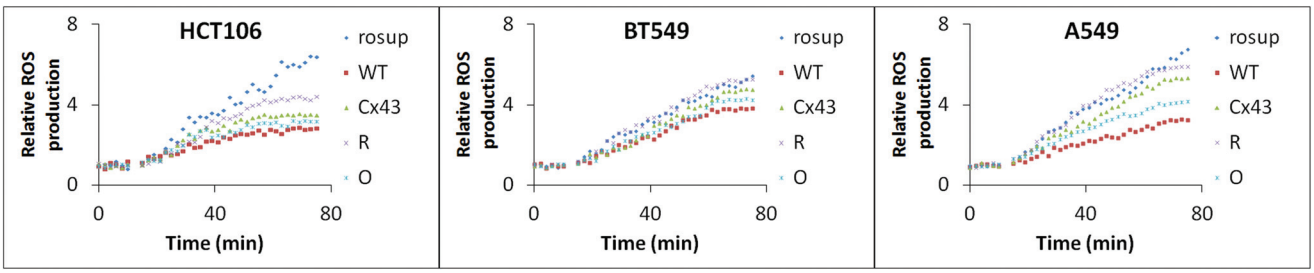

Fig. 5 Effect of GJIC function on ROS production during cisplatin treatments in HCT106, BT549 and A549 cells. The data showed kinetics of ROS production in cells as a function of time. Cells were incubated for 30 min in the presence of DCFH-DA, washed and their fluorescence was measured every 2 min for a negative control period of 10 min. There is no data at the time between 10 min and 15 min because time was needed to add cisplatin to the medium. A positive control was obtained by adding 0.1 mg mL^{-1} of rosup as an external oxidant molecule. The groups of "R" and "O" were the cells, which were pretreated with retinoic acid (10 μM) for 24 h or oleamide (25 μM) for 1 h before the assay. All data were normalized by the mean value of data in the negative control period.

results of the Student's *t* test. Briefly, GJIC enhances cytotoxicity in cells that have a higher "Max" in Cx43-transfected cells than WT. The following apoptosis state can also be evaluated by SPR signal curves.

In the second stage, the RU decline may be mainly caused by caspase-3 activation. Cisplatin treatment can increase caspase-8 and caspase-9 activity, which can be both regulated by oleamide and retinoic acid.[28] Activation of caspase-8 and caspase-9 can both activate caspase-3, resulting in morphological changes[44] that relate to RIU. The level of caspase-3 activation is also affected by GJIC function, and these activation level differences relate to different morphological changes, which are associated with RU decline. In addition, for the analysis of "Decline" values, a control group (no cisplatin treatment) of each cell line was used to evaluate the influence of SPR measurement on cells, and the RU variations of the three control groups were all less than 0.8 RU, which is very low compared with the values of other groups. Thus, the influence of SPR measurement on cells is too small to affect the results.

The cytotoxicity of anti-tumor drugs is always affected by tumor-suppressor gene expression,[45] and the cytotoxicity of cisplatin is also affected by Cx43 expression.[29] The mechanism can be conveniently determined by real-time monitoring of the whole reaction with no lost information which is always lost in conventional biological methods. In this study, a SPR biosensor with real-time detection ability was used to evaluate the effect of Cx43 expression or GJIC function on cisplatin cytoxicity. It was found that the adjustment of Cx43 expression mainly affected the SPR signal at the time of oxidative stress. This suggests that Cx43 expression may enhance the oxidative stress caused by cisplatin in these three cell lines, and whether Cx43 expression enhances or reduces cisplatin cytotoxicity in

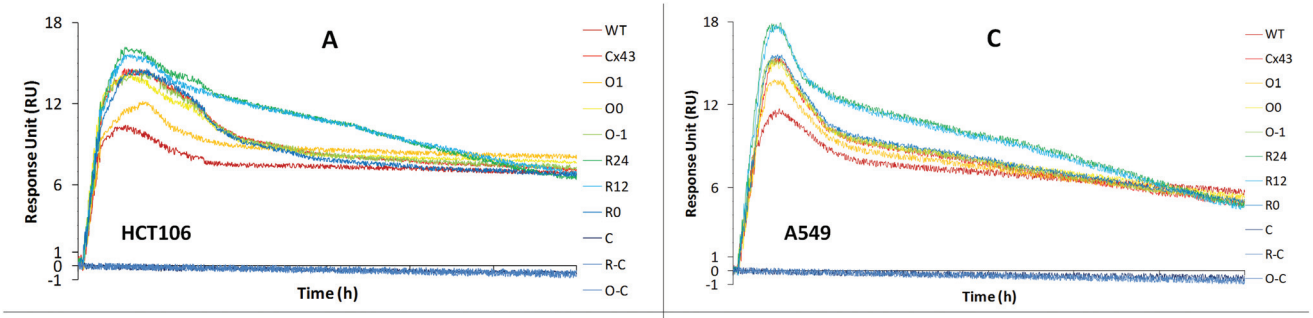

D

Cell line	HCT106		BT549		A549	
Cell type	Max	Decline	Max	Decline	Max	Decline
WT	10.4	3.69	9.28	5.52	11.72	6.05
Cx43	14.6*	7.46*	10.42*	7.91*	15.35*	10.43*
O1	12.14*	4.2*	9.77*	6.02*	13.81*	8.8*
O0	14.33	6.73*	10.15	7.22	15.15	9.83*
O-1	14.53	7.24	10.22	7.27	15.45	10.39
R24	16.15*	9.46*	12.66*	9.69*	17.84*	12.99*
R12	15.61	8.75*	12.41*	9.46*	17.73*	13.07*
R0	14.57	7.82	10.78	8.7	15.61	10.47
C		0.6		0.75		0.47

Fig. 6 SPR measurement results. The response of the three cell lines to cisplatin was measured. Oleamide (O) or retinoic acid (R) was added at three time points before cisplatin treatment. Two values were determined for analyses: the RU peak value ("Max") and the difference between "Max" and RU at 6 h ("Decline"). C: control group, cells with no cisplatin treatment. R–C: cells treated by retinoic acid. O–C: cells treated by oleamide. (A) HCT106 cell line; (B) BT549 cell line; (C) A549 cell line; (D) Analysis of results. Differences between groups were identified using the Student's *t* test; Cx43 transfection was compared with WT, oleamide treatment was compared with Cx43 transfection, and retinoic acid treatment was compared with Cx43 transfection. The results of "R–C" and "O–C" were similar to the results of "C", so they are not listed in the table. *$P < 0.05$. When "Decline" values were used for comparison, all "Decline" values were subtracted from the value of control group.

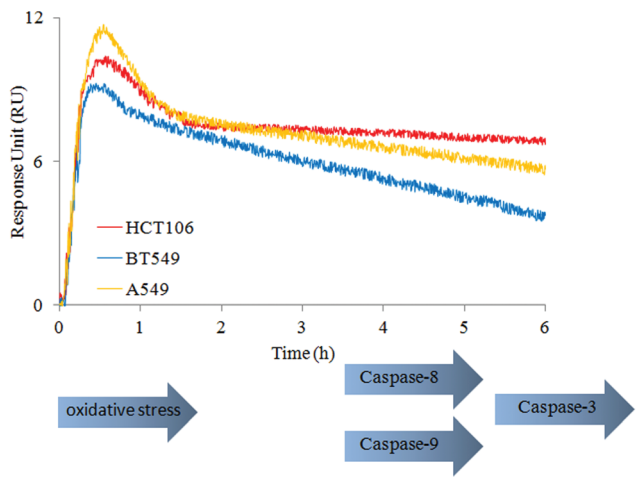

Fig. 7 The relationship between SPR signal curves and cellular response to cisplatin in three cell lines. The rapid changes of RU within the first hour occur at the same time as oxidative stress is induced by cisplatin. The slow decline of RU is caused by morphologic changes that relate to caspase-3 activation.

other cells can be also determined by the "Max" value. Thus, this work provides a real-time and fast detection method to determine how the expression of a tumor related gene affects the cytotoxicity of an anti-tumor drug, which is important in the mechanism of drug resistance.

Evaluating cellular responses to drugs is crucial for chemotherapy[46] and drug screening.[47] Several methods have been used for detecting cellular responses to drugs, including western blot, cell viability assays, immunofluorescence, and flow cytometry. But these methods only detect a certain protein or index. The SPR biosensor provides the RIU variations of cells in real time. Comparison of the results of this study with the results of the traditional biological methods shows that the SPR biosensor can provide the overall status of the integral cell. Some studies have proved that the RIU variations are related to a certain index[48] when cells are treated by a certain agent. In this study, the RIU variations were proved to be related to cellular responses to cisplatin. This suggests that the RIU of cells may be a useful reference index to supplement the lack of biological methods in therapeutic evaluation of anticancer drugs.

5 Conclusions

The real-time detection ability of SPR biosensors is a powerful tool to monitor the entire process of the cellular response to drugs to determine cytotoxicity mechanisms. In this work, the responses of three cancer cell lines to cisplatin were measured using a phase-modulated SPR sensor with a 7.25×10^{-6} RIU stability at 6 h and 10^{-6} RIU sensitivity, to determine the effect

of Cx43 expression on cisplatin cytotoxicity. Traditional biological assays and SPR biosensor measurements both showed that Cx43 expression can enhance cisplatin cytotoxicity in these cell lines. Analyses of SPR signal curves further confirmed that Cx43 expression can enhance the oxidative stress induced by cisplatin. These results suggest that the SPR biosensor can be a useful tool to determine the influence factors and mechanisms of drug cytotoxicity by its real-time detection ability.

Acknowledgements

This work was partially supported by the Foundation of Tianjin Health Bureau under Grant number 2014KY27, and the foundation of committee on science and technology of Tianjin under Grant numbers 15JCQNJC42200 and 13JCYBJC42700, and the National Natural Science Foundation of China under Grant numbers 81472729, 81503127, 61138003 and 61427819, XY acknowledges support from the Ministry of Science and Technology of China under National Basic Research Program of China (973) Grant number 2015CB352004 and the start-up funding at Shenzhen University.

Notes and references

1 V. Chabot, C. M. Cuerrier, E. Escher, V. Aimez, M. Grandbois and P. G. Charette, Biosensing based on surface plasmon resonance and living cells, *Biosens. Bioelectron.*, 2009, **24**, 1667.
2 Y. J. Wang, C. L. Zhang, Y. Q. Zhang, H. Fang, C. J. Min, S. W. Zhu and X. C. Yuan, Investigation of phase SPR biosensor for efficient targeted drugscreening with high sensitivity and stability, *Sens. Actuators, B*, 2015, **209**, 313.
3 R. Z. Yusuf, Z. Duan, D. E. Lamendola, R. T. Penson and M. V. Seiden, Paclitaxel Resistance: Molecular Mechanisms and Pharmacologic Manipulation, *Curr. Cancer Drug Targets*, 2003, **3**, 1.
4 R. A. Weinberg, Tumor suppressor genes, *Science*, 1991, **254**, 1138.
5 T. J. King and J. S. Bertram, Connexins as targets for cancer chemoprevention and chemotherapy, *Biochim. Biophys. Acta*, 2005, **1719**, 146.
6 A. L. Harris, Emerging issues of connexin channels: biophysics fills the gap, *Q. Rev. Biophys.*, 2001, **34**, 325e472.
7 K. Willecke, J. Eiberger, J. Degen, D. Eckardt, A. Romualdi, M. Guldenagel, U. Deutsch and G. Sohl, Structural and functional diversity of connexin genes in the mouse and human genome, *Biol. Chem.*, 2002, **383**, 725.
8 J. C. Saez, V. M. Berthoud, M. C. Branes, A. D. Martinez and E. C. Beyer, Plasma membrane channels formed by connexins: their regulation and functions, *Physiol. Rev.*, 2003, **83**, 1359.
9 H. Yamasaki and C. Naus, Role of connexin genes in growth control, *Carcinogenesis*, 1996, **17**, 1199.
10 X. Hong, Q. Wang, Y. Yang, S. Zheng, X. Tong, S. Zhang, L. Tao and A. L. Harris, Gap junctions propagate opposite effects in normal and tumor testicular cells in response to cisplatin, *Cancer Lett.*, 2012, **317**, 165.
11 B. He, X. Tong, L. Wang, Q. Wang, H. Ye, B. Liu, X. Hong, L. Tao and A. L. Harris, Tramadol and flurbiprofen depress the cytotoxicity of cisplatin via their effectson gap junctions, *Clin. Cancer Res.*, 2009, **15**, 5803.
12 T. Huang, Y. Zhu, X. Fang, Y. Chi, M. Kitamura and J. Yao, Gap junctions sensitize cancer cells to proteasome inhibitor MG132-induced apoptosis, *Cancer Sci.*, 2010, **101**, 713.
13 L. Kelsey, P. Katoch, K. E. Johnson, S. K. Batra and P. P. Mehta, Retinoids regulatethe formation and degradation of gap junctions in androgen-responsive human-prostate cancer cells, *PLoS One*, 2012, **7**, e32846.
14 O. Kucuk, F. H. Sarkar, W. Sakr, Z. Djuric, M. N. Pollak, F. Khachik, Y. W. Li, M. Banerjee, D. Grignon, J. S. Bertram, J. D. Crissman, E. J. Pontes and D. P. Wood, Phase II randomized clinical trial of lycopene supplementation before radical prostatectomy, *Cancer Epidemiol., Biomarkers Prev.*, 2001, **10**, 861.
15 H. Guo, P. Acevedo, F. D. Parsa and J. S. Bertram, Gap-junctional protein connexin 43 is expressed in dermis and epidermis of human skin: differential modulation by retinoids, *J. Invest. Dermatol.*, 1992, **99**, 460.
16 L. X. Zhang, R. V. Cooney and J. S. Bertram, Carotenoids enhance gap junctional communication and inhibit lipid peroxidation in C3H/10T1/2 cells: relationship to their cancer chemopreventive action, *Carcinogenesis*, 1991, **12**, 2109.
17 R. Huang, M. Z. Hossain, R. Huang, J. Gano, Y. Fan and A. L. Boynton, Connexin 43 (cx43) enhances chemotherapy-induced apoptosis in human glioblastoma cells, *Int. J. Cancer*, 2001, **92**, 130.
18 J. L. Munoz, C. V. Rodriguez, S. J. Greco, S. H. Ramkissoon, K. L. Ligon and P. Rameshwar, Temozolomide resistance in glioblastoma cells occurs partly through epidermal growth factor receptor mediated induction of connexin 43, *Cell Death Dis.*, 2014, **5**, e1145.
19 Y. J. Kim, J. Kim, C. Tian, H. J. Lim, Y. S. Kim, J. H. Chung and Y. H. Choung, Prevention of cisplatin-induced ototoxicity by the inhibition of gap junctional intercellular communication in auditory cells, *Cell. Mol. Life Sci.*, 2014, **71**, 3859.
20 J. Chang, H. Wang, X. Wang, Y. Zhao, D. Zhao, C. Wang, Y. Li, Z. Yang, S. Lu, Q. Zeng, J. Zimmerman, Q. Shi, Y. Wang and Y. Yang, Molecular mechanisms of Polyphyllin I-induced apoptosis and reversal of the epithelial-mesenchymal transition in human osteosarcoma cells, *J. Ethnopharmacol.*, 2015, **170**, 117.
21 B. He, H. Tao, S. Liu and A. Wei, Protective effect of carboxymethylated chitosan on hydrogen peroxide-induced apoptosis in nucleus pulposus cells, *Mol. Med. Rep.*, 2015, **11**, 1629–1638.

22 D. C. Duffy, J. C. McDonald, O. J. Schueller and G. M. Whitesides, Rapid prototyp-ing of microfluidic systems in poly(dimethylsiloxane), *Anal. Chem.*, 1998, **70**, 4974.

23 J. K. Zhang, L. Yang, G. L. Meng, J. Fan, J. Z. Chen, Q. Z. He, S. Chen, J. Z. Fan, Z. J. Luo and J. Liu, Protective effect of tetrahydroxystilbene glucoside against hydrogen peroxide-induced dysfunction and oxidative stress in osteoblastic MC3T3-E1 cells, *Eur. J. Pharmacol.*, 2012, **689**, 31.

24 S. Lee, D. L. Paul, K. Keyomarsi and R. Sager, Transcriptional downregulation of gap junction proteins blocks junctional communication in human mammary tumor cell lines, *J. Cell Biol.*, 1992, **118**, 1213.

25 C. K. Cesen, M. J. Fernstrom, A. M. Malkinson and R. J. Ruch, Frequent reduction of gap junctional intercellular communication and connexin 43 expression in human and mouse lung carcinoma cells, *Carcinogenesis*, 1998, **19**, 61.

26 S. Solveig, B. Jarle, K. Matthias, A. Kjenseth, G. E. Lind, A. Svindland, A. Brech, A. Nesbakken, R. A. Lothe, E. Leithe and E. Rivedal, Connexin 43 acts as a colorectal cancer tumor suppressor and predicts disease outcome, *Int. J. Cancer*, 2012, **131**, 570.

27 S. T. P. Bernard, Cisplatin in cancer therapy: Molecular mechanisms of action, *Eur. J. Pharmacol.*, 2014, **740C**, 364.

28 S. Kaori, M. Takashi, A. Yoshihiro, Y. Yuji, S. Hodaka and S. Masaki, Connexin 43 transfection in basaloid squamous cell carcinoma cells, *Oncol. Rep.*, 2006, **16**, 285.

29 H. Sato, H. Iwata, Y. Takano, R. Yamada, H. Okuzawa, Y. Nagashima, K. Yamaura, K. Ueno and T. Yano, Enhanced effect of connexin 43 on cisplatin-induced cytotoxicity in mesothelioma Cells, *J. Pharmacol. Sci.*, 2009, **110**, 466.

30 X. H. Tong, S. Y. Dong, M. L. Yu, Q. Wang and L. Tao, Role of heteromeric gap junctions in the cytotoxicity of cisplatin, *Toxicology*, 2013, **310**, 53.

31 A. G. Porter and R. U. Janicke, Emerging roles of caspase-3 in apoptosis, *Cell Death Differ.*, 1999, **6**, 99.

32 K. H. Lu, K. H. Lue, M. C. Chou and J. G. Chung, Paclitaxel induces apoptosis via caspase-3 activation in human osteogenic sarcoma cells (U-2 OS), *J. Orthop. Res.*, 2005, **23**, 988.

33 M. Xu, M. Takanashi, K. Oikawa, M. Tanaka, H. Nishi, K. Isaka, M. Kudo and M. Kuroda, USP15 plays an essential role for caspase-3 activation during Paclitaxel-induced apoptosis, *Biochem. Biophys. Res. Commun.*, 2009, **388**, 366.

34 X. J. Wu, Y. Q. Zhang, C. J. Min, S. W. Zhu, J. Feng and X.-C. Yuan, *Laser Phys. Lett.*, 2013, **10**, 065604.

35 J. Guck, S. Schinkinger, B. Lincoln, F. Wottawah, S. Ebert, M. Romeyke, D. Lenz, H. M. Erickson, R. Ananthakrishnan, D. Mitchell, J. Kas, S. Ulvick and C. Bilby, Optical deformability as an inherent cell marker for testing malignant transformation and metastatic competence, *Biophys. J.*, 2005, **88**, 3689.

36 O. Otto, P. Rosendahl, A. Mietke, S. Golfier, C. Herold, D. Klaue, S. Girardo, S. Pagliara, A. Ekpenyong, A. Jacobi, M. Wobus, N. Töpfner, U. F. Keyser, J. Mansfeld, E. Fischer-Friedrich and J. Guck, Real-time deformability cytometry: on-the-fly cell mechanical phenotyping, *Nat. Methods*, 2015, **12**, 199.

37 S. Y. Wu, H. P. Ho, W. C. Law and C. Lin, Highly sensitive differential phase-sensitive surface plasmon resonance biosensor based on the Mach-Zehnder configuration, *Opt. Lett.*, 2004, **29**, 2378.

38 R. Robelek and J. Wegener, Label-free and time-resolved measurements of cell volume changes by surface plasmon resonance (SPR) spectroscopy, *Biosens. Bioelectron.*, 2010, **25**, 1221.

39 F. Liu, J. Zhang, Y. Deng, D. Wang, Y. Lu and X. Yu, Detection of EGFR on living human gastric cancer BGC823 cells using surface plasmon resonance phase sensing, *Sens. Actuators, B*, 2011, **153**, 398.

40 T. Y. Nakamura, I. Yamamoto, Y. Kanno, Y. Shiba and K. Goshima, Metabolic coupling of glutathione between mouse and quail cardiac myocytes and its protective role against oxidative stress, *Circ. Res.*, 1994, **74**, 806.

41 B. Jamali, M. Nakhjavani, L. Hosseinzadeh, S. N. Nikounezhad and H. S. Farshad, Intracellular GSH Alterations and Its Relationship to Level of Resistance following Exposure to Cisplatin in Cancer Cells, *Iran. J. Pharm. Res.*, 2015, **14**, 513.

42 V. A. Krutovskikh, C. Piccoli and H. Yamasaki, Gap junction intercellular communication propagates cell death in cancerous cells, *Oncogene*, 2002, **21**, 1989.

43 S. Al-Bahlani, M. Fraser, A. Y. C. Wong, B. S. Sayan, R. Bergeron, G. Melino and B. K. Tsang, P73 regulates cisplatin-induced apoptosis in ovarian cancer cells via a calcium/calpain-dependent mechanism, *Oncogene*, 2011, **30**, 4219.

44 K. C. Zimmermann, C. Bonzon and D. R. Green, The machinery of programmed cell death, *Pharmacol. Ther.*, 2001, **92**, 57.

45 H. C. Tsai, C. Y. Huang, H. L. Su and C. H. Tang, CTGF increases drug resistance to paclitaxel by upregulating surviving expression in human osteosarcoma cells, *Biochim. Biophys. Acta*, 2014, **1843**, 846.

46 D. B. Zamble and S. J. Lippard, Cisplatin and DNA repair in cancer chemotherapy, *Trends Biochem. Sci.*, 1995, **20**, 435.

47 M. Fryknas, J. Gullbo, X. Wang, L. Rickardson, M. Jarvius, M. Wickstrom, S. Hassan, C. Andersson, M. Gustafsson, G. Westman, P. Nygren, S. Linder and R. Larsson, *BMC Cancer*, 2013, **13**, 374.

48 T. Hiragun, Y. Yanase, K. Kose, T. Kawaguchi, K. Uchida, S. Tanaka and M. Hide, Surface plasmon resonance-biosensor detects the diversity of responses against epidermal growth factor in various carcinoma cell lines, *Biosens. Bioelectron.*, 2012, **32**, 202.

